Consistent nuclear matter calculations with local three-nucleon interactions

Domenico Logoteta
Department of Physics, University of Pisa, and INFN, Sezione di Pisa, Largo B. Pontecorvo 3, I-56127 Pisa, Italy

(Received 3 June 2019; published 10 October 2019)

I calculate the energy per particle of symmetric nuclear matter and pure neutron matter in the framework of the microscopic Brueckner-Hartree-Fock approach using some recent interactions derived in chiral perturbation theory at next-to-next-to-next-to-leading order (N3LO) for the nucleon-nucleon (NN) force, and next-to-next-to-leading order (N2LO) for the nucleon-nucleon-nucleon (NNN) one. The interactions considered in the present work have been adjusted to properties of light nuclei with $A = 3$, adopting local regulators for the NNN interaction. I performed several calculations using an effective density dependent two-body force obtained from the original NNN one keeping the same parameters and the same regularization scheme employed in finite light nuclei calculations; I then compared these results with other calculations obtained, retaining the same parameters of the NNN force fixed on light nuclei but using a nonlocal regulator. This second strategy has been often used in the literature due to the easier derivation of the effective NN force in this case. I found that in pure neutron matter the use of local or nonlocal regulators does not sensibly affect the calculation of the energy per particle while in symmetric nuclear matter the use of local or nonlocal regulators produces appreciable differences. Saturation properties of nuclear matter are discussed for the various models considered; the uncertainties on the reported calculations are also estimated.

DOI: 10.1103/PhysRevC.100.045803

I. INTRODUCTION

The description of systems made of strongly interacting nucleons such as finite nuclei and nuclear matter based on microscopic approaches requires an accurate knowledge of nuclear interactions. The effective field theory (EFT) for low-energy quantum chromodynamics (QCD) [1] outlines a powerful way to derive consistent nuclear interactions (for a review on this subject see Refs. [2–5]). This method allows to calculate perturbatively the interactions between nucleons (two- as well as many-body interactions) according to a well defined scheme based on an effective QCD Lagrangian constructed in such a way to retain the main symmetries of QCD, and in particular the approximate chiral symmetry.

Such a systematic procedure is very powerful for nuclear systems where the importance of the three-nucleon forces is a well established feature [6–8].

Nucleon-nucleon (NN) interactions plus nucleon-nucleon-nucleon (NNN) forces based on chiral perturbation theory (ChPT) have been used to investigate properties of light nuclei [9], nuclei with $A \leqslant 18$ [10], medium-mass nuclei [11–13], and heavy nuclei [14]. An important task in this line is the evaluation of the uncertainties originating in the nuclear Hamiltonian [15] and in particular in the so-called low-energy constants (LECs).

In this work, I present some microscopic calculations of the equation of state (EOS) of symmetric nuclear matter (SNM) and pure neutron matter (PNM) using the chiral potentials derived in Ref. [16] up to next-to-next-to-next-to-next-to-leading order (N4LO) of ChPT. However, since the treatment of NNN force is limited to next-to-next-to-leading order (N2LO) [17], I use NN potential up to next-to-next-to-next-to-leading order (N3LO) as is often done in literature. I also discuss the important contributions of NNN forces at N3LO. Present many-body calculations are based on the Brueckner-Bethe-Goldstone (BBG) [18,19] theory within the Brueckner-Hartree-Fock (BHF) approximation. In some previous works [20–22] I employed two-body interactions at N3LO of ChPT plus three-nucleon forces at N2LO, finding that in some cases it was possible to simultaneously reproduce satisfactory properties of nuclear matter and light nuclei. In this work I perform a similar analysis but consider a more consistent treatment of the regulator in the NNN force which is kept in local form as used in recent few-body nuclei calculations based on the hyperspherical harmonics approach to fix the values of the LECs in the nuclear Hamiltonian. Such a consistent treatment of the regulator in the NNN force was implemented in Ref. [23] in the case of very simple three-nucleon forces.

Several groups calculated the EOS of PNM [24–31] and SNM [32–37] and many efforts are currently devoted to improving the accuracy of the many-body techniques as well as to try to include in numerical calculations very complicated nuclear interactions.

The paper is organized as follows: in the first section I discuss the two- and three-body chiral interactions used in present calculations; in the second section I briefly review the basic features of the BBG many-body theory and the inclusion of NNN force in the BHF approach; the third section is devoted to showing the results of present calculations; and finally in the last section I summarize the main results and outline conclusions of the present work.

II. CHIRAL NUCLEAR INTERACTIONS

The interactions considered in the present work were derived in ChPT both for the two- and three-nucleon

TABLE I. Values of the LECs used in the present calculations according to the order of the expansion in ChPT and to the cutoff value Λ. The LECs c_1, c_3, and c_4 are expressed in GeV^{-1}, whereas c_D and c_E are dimensionless. The values in parentheses are the errors arising from the fitting procedure (see Ref. [47]).

Order (Λ)	c_D	c_E	c_1	c_3	c_4
N2LO (450)	0.935(0.215)	0.12(0.04)	−0.74	−3.61	2.44
N2LO (500)	0.495(0.195)	−0.07(0.04)	−0.74	−3.61	2.44
N3LO (450)	0.675(0.205)	0.31(0.05)	−1.07	−5.54	4.17
N3LO (500)	−0.945(0.215)	−0.68(0.04)	−1.07	−5.54	4.17
N3LO+2π (450)	0.670(0.210)	0.41(0.05)	−1.20	−4.43	2.67
N3LO+2π (500)	−0.750(0.210)	−0.41(0.04)	−1.20	−4.43	2.67

interactions. I use indeed *NN* potentials calculated at the N3LO of ChPT, in conjunction with *NNN* interactions calculated at N2LO. Currently, chiral *NN* potentials have been calculated up to N4LO by Epelbaum *et al.* [38] and by Entem *et al.* [16]. In addition, dominant contributions at next-to-next-to-next-to-next-to-next-to-leading order (N5LO) were analyzed in Ref. [39] where a satisfactory convergence of the perturbative expansion of the *NN* potential was found. Recently Piarulli *et al.* [40] developed a fully local-in-coordinate-space two-nucleon chiral potential which includes the Δ isobar intermediate state at N3LO. This new potential represents the fully local version of the minimally nonlocal chiral interaction reported in Ref. [41]. Similarly to the case of *NN* interaction, also *NNN* forces have been calculated at higher order in the chiral low-energy expansion. Subleading contributions appear first at N3LO; however, the number of LECs is unchanged at this order compared to N2LO. Ten new purely *NNN* LECs appear at N4LO [42]. The inclusion of these contributions may be potentially important to get an improved accuracy of the *NNN* interaction. Owing to their complexity, the use of these forces in practical calculations is not an easy task and the inclusion of part of these interactions in studies of few- and many-body systems is currently a very active research field.

I focus now on the specific interactions that I have employed in the present work. As a two-body nuclear interaction, I used the potentials calculated at N3LO proposed in Ref. [16]. The authors of Ref. [16] provided three different versions of the two-body interactions according to three values of the cutoff, $\Lambda = 450$, 500, and 550 MeV, used to regularize the short-range part of the potentials. An interesting feature of these new *NN* potentials is that the obtained χ^2/datum was 1.15 for $\Lambda = 500$ MeV and just slightly larger for $\Lambda = 450$ MeV which is a very remarkable result compared to other interactions.

In the construction of the *NN* potential, the authors of Ref. [16] applied the same power counting scheme as well as the same cutoff procedures at all orders. Moreover, the long-range parts of these potentials have been fixed by the very accurate πN LECs as determined in Ref. [43] which essentially lead to very small uncertainties in the variation of the associated values. This strongly reduced the propagated uncertainties in the *NN* interaction.

It is worth noting that at N2LO of ChPT arise all the possible operators contributing to the *NN* potential as well as the leading-order *NNN* forces. The *NNN* force that I employed is calculated up to N2LO, and is fitted in Ref. [44] to reproduce the binding energy of ^{3}H as well as the Gamow-Teller matrix element in ^{3}H β-decay using the two-body potentials of Ref. [16]. The N3LO + N2LO interactions described above were used in Ref. [45] to calculate the momentum distribution function in $A = 3$ nuclei.

Concerning the *NNN* force at N2LO, it is of the form derived by Epelbaum *et al.* [17] with the difference that the regulator used in Refs. [44,45] is local. I note that the nonlocality of the N2LO three-nucleon interaction depends only on the functional form of the regulator used. The N2LO *NNN* force has the following structure in momentum space:

$$V_{NNN}^{(2\pi)} = \sum_{i\neq j\neq k} \frac{g_A^2}{8f_\pi^4} \frac{\boldsymbol{\sigma}_i\cdot\boldsymbol{q}_i\,\boldsymbol{\sigma}_j\cdot\boldsymbol{q}_j}{(\boldsymbol{q}_i^2+m_\pi^2)(\boldsymbol{q}_j^2+m_\pi^2)} F_{ijk}^{\alpha\beta}\tau_i^\alpha\tau_j^\beta, \quad (1)$$

$$V_{NNN}^{(1\pi)} = -\sum_{i\neq j\neq k} \frac{g_A c_D}{8f_\pi^4\Lambda_\chi} \frac{\boldsymbol{\sigma}_j\cdot\boldsymbol{q}_j}{\boldsymbol{q}_j^2+m_\pi^2} \boldsymbol{\sigma}_i\cdot\boldsymbol{q}_j\,\boldsymbol{\tau}_i\cdot\boldsymbol{\tau}_j, \quad (2)$$

$$V_{NNN}^{(\mathrm{ct})} = \sum_{i\neq j\neq k} \frac{c_E}{2f_\pi^4\Lambda_\chi} \boldsymbol{\tau}_i\cdot\boldsymbol{\tau}_j, \quad (3)$$

where $\boldsymbol{q}_i = \boldsymbol{p}_i' - \boldsymbol{p}_i$ is the difference between the final and initial momenta of nucleon i and

$$F_{ijk}^{\alpha\beta} = \delta^{\alpha\beta}\left(-4c_1m_\pi^2 + 2c_3\boldsymbol{q}_i\cdot\boldsymbol{q}_j\right) + c_4\epsilon^{\alpha\beta\gamma}\tau_k^\gamma\boldsymbol{\sigma}_k\cdot(\boldsymbol{q}_i\times\boldsymbol{q}_j). \quad (4)$$

In Eqs. (1)–(4) $\boldsymbol{\sigma}_i$ and $\boldsymbol{\tau}_i$ are Pauli matrices for spin and isospin spaces while $g_A = 1.29$ and $f_\pi = 92.4$ MeV are the axial-vector coupling and the pion decay constant. The nucleon labels i, j, and k can take values 1, 2, and 3, which results in six possible permutations in each sum. Factors c_1, c_3, c_4, c_D, and c_E are low-energy constants. I note that the constants c_1, c_3, and c_4 in Eq. (4), coming from the πN Lagrangian, are already fixed at the two-body level. The remaining parameters c_D and c_E are not determined by the two-body interaction and have to be fixed constraining some specific observable of few-body nuclear systems as discussed previously. One of the sources of uncertainty of the nuclear Hamiltonian concerns the choice of the observables used to fix c_E and c_D. Since two parameters have to be fixed, the value of two different observables is necessary. A possibility is to use the binding energy of the ^{3}H in conjunction with the *nd* scattering length, the binding energy of ^{4}He, the charge radius of ^{4}He, and, as I stated before, the Gamow-Teller matrix element in ^{3}H β-decay. The values of the constants c_i for the interactions that I consider in the present work are reported in Table I. The values in parentheses indicate the errors arising from the fitting procedure as reported in Refs. [44,45]. However, I checked that the small uncertainties associated to the fit error have negligible effects on present calculations. I note that it was very recently discovered [46] that in the derivation of chiral effective field theory (ChEFT) currents a factor of $-1/4$ was missing from the one-pion exchange term in the *NNN* force. This affected the fit of the low-energy constant c_D entering in the ^{3}H half-life calculation, and thus also all previous nuclear matter calculations using these values were affected by the same problem. This issue was recently fixed

[47] and therefore the calculations presented in this work are correct.

To try to estimate the theoretical uncertainties of the reported calculations I performed a variation of the values of the LECs and employed different cutoff values, namely, $\Lambda = 450$ and 500 MeV. I also tried to estimate the error associated to the truncation of the *NNN* expansion to N2LO by evaluating the 2π-exchange contributions up to N3LO. I note that the 2π-exchange contributions are just one particular topology present in the *NNN* force at N3LO; thus its inclusion in the many-body calculations should be intended as an attempt to get only an estimate of the size of a typical contribution at this order. A more in-depth and quantitative study clearly requires the inclusion of the full N3LO *NNN* force and will be the subject of a future work. All the previous uncertainties are related to ChEFT. There are other uncertainties that should be addressed to the many-body method used, namely, the BHF approach in the present case. These issues are discussed in the last part of the paper.

To regularize the *NNN* force, I considered both local regulator (LR) and nonlocal regulator (NLR) functions of the form

$$F_{LR}(\Lambda) = \exp\left[-\left(\frac{(\boldsymbol{p}-\boldsymbol{p}')^4}{\Lambda^4}\right)\right], \tag{5}$$

$$F_{NLR}(\Lambda) = \exp\left[-\left(\frac{p^4-p'^4}{\Lambda^4}\right)\right]. \tag{6}$$

I note that $F_{LR}(\Lambda)$ is consistent with the *NNN* force used in Ref. [44] to fix the low-energy constants c_E and c_D.

I also observe that, adopting $F_{NLR}(\Lambda)$ which is symmetric under the exchange of particle indices, the low energy constants c_E and c_D give vanishing contributions in PNM for symmetry reasons. Using instead $F_{LR}(\Lambda)$ terms proportional to c_E and c_D give nonvanishing contributions also in PNM [48].

III. THE BHF APPROACH WITH AVERAGED THREE-BODY FORCES

The BHF approach is the leading order of the BBG many-body theory [18,19]. In such a theory, the ground state energy of nuclear matter is calculated in terms of the so-called hole-line expansion, where diagrams are grouped according to the number of independent hole lines. This expansion is derived using the in-medium two-body scattering Brueckner *G*-matrix which represents the effective nucleon-nucleon interaction in the presence of the surrounding medium. In the case of asymmetric nuclear matter with neutron density ρ_n, proton density ρ_p, total nucleon density $\rho = \rho_n + \rho_p$, and isospin asymmetry $\beta = (\rho_n - \rho_p)/\rho$, one has different *G*-matrices describing the *nn*, *pp*, and *np* in-medium effective interactions. They are obtained by solving the well known Bethe-Goldstone equation, written schematically as

$$G_{\tau\tau'}(\omega) = V_{\tau\tau'} + \sum_{k,k'} V_{\tau\tau'} \frac{|\boldsymbol{k},\boldsymbol{k}'\rangle\, Q_{\tau\tau'}\, \langle \boldsymbol{k},\boldsymbol{k}'|}{\omega - \epsilon_\tau(k) - \epsilon_{\tau'}(k') + i\varepsilon} G_{\tau\tau'}(\omega)\,, \tag{7}$$

where $\tau, \tau' = n, p$ are isospin indices, $V_{\tau\tau'}$ denotes the bare *NN* interaction in a given channel, and $|\boldsymbol{k},\boldsymbol{k}'\rangle\, Q_{\tau\tau'}\, \langle \boldsymbol{k},\boldsymbol{k}'|$ is the Pauli operator which projects out the intermediate nucleon states of the Fermi sphere. In this way the Pauli exclusion principle is automatically satisfied. ω is the so-called starting energy which corresponds to the sum of nonrelativistic energies of the interacting nucleons. The single-particle energy ϵ_τ of a nucleon with momentum k and mass m_τ is given by

$$\epsilon_\tau(k) = \frac{\hbar^2 k^2}{2m_\tau} + U_\tau(k), \tag{8}$$

where the single-particle potential $U_\tau(k)$ represents the mean field felt by a nucleon due to its interaction with the other nucleons. In the BHF approximation, $U_\tau(k)$ is calculated through the real part of the so-called on-shell *G*-matrix, and is given by

$$U_\tau(k) = \sum_{\tau'=n,p} \sum_{k' \leqslant k_{F_{\tau'}}} \mathrm{Re}\langle \boldsymbol{k}\boldsymbol{k}'|G_{\tau\tau'}(\omega = \omega^*)|\boldsymbol{k}\boldsymbol{k}'\rangle_A, \tag{9}$$

where $\omega^* = \epsilon_\tau(k) + \epsilon_{\tau'}(k')$ and the sum runs over all neutron and proton occupied states and the matrix elements are antisymmetrized. I make use of the so-called continuous choice [49–52] for the single-particle potential $U_\tau(k)$ when solving the Bethe-Goldstone equation. As shown in Refs. [53,54], the contribution of the three-hole-line diagrams to the energy per particle, E/A, is minimized in this prescription and thus a faster convergence of the hole-line expansion for E/A is achieved [53–55] with respect to the so-called standard choice for $U_\tau(k)$.

In numerical calculations a self-consistent solution of Eqs. (7)–(9) is required; once this is reached, the energy per particle is given by

$$\frac{E}{A}(\rho,\beta) = \frac{1}{A} \sum_{\tau=n,p} \sum_{k \leqslant k_{F_\tau}} \left(\frac{\hbar^2 k^2}{2m_\tau} + \frac{1}{2} U_\tau(k)\right). \tag{10}$$

I note that in the present paper I do not make use of the so-called parabolic approximation in the single particle potentials $U_\tau(k)$. Such an approximation introduces indeed additional uncertainties in the choice of the two momenta needed to evaluate the single particle spectrum. I therefore calculated $U_\tau(k)$ using a grid with 32 points in a fully self-consistent way.

Inclusion of three-nucleon forces in the BHF approach

The reproduction of the empirical saturation point of symmetric nuclear matter, $\rho_0 = 0.16 \pm 0.01$ fm^{-3}, $E/A|_{\rho_0} = -16.0 \pm 1.0$ MeV, is not possible when using a two-body nuclear interaction only. The saturation points obtained using different *NN* potentials lie indeed within the so-called Coester band [56,57], with either a too large saturation density or a too small binding energy ($B = -E/A$) compared to the empirical values. Several works have shown that SNM results are over-bound with a too large saturation density when using modern high precision *NN* potentials, fitting *NN* scattering data up to energies of 350 MeV, with a χ^2 per datum close to 1 [58]. As for few-nucleon systems [6–8], also for the case of nuclear matter *NNN* forces are considered an important

missing physical mechanism. The inclusion of *NNN* force is thus required in order to reproduce a realistic saturation point of SNM [59–64].

Within the BHF approach *NNN* forces cannot be used directly in their original form. This would require to solve three-body Faddeev equations in the medium (Bethe-Faddeev equations) [65,66] and currently this is a very hard task. To circumvent this problem an effective density dependent two-body force is built starting from the original three-body one by properly averaging over one of the three nucleons [67–69].

In the present work, I consider three different approximations in the in-medium effective *NN* force (hereafter $V_{\rm eff}$). The first approximation was discussed in Ref. [69], where $V_{\rm eff}$ was derived by closing one of the three fermion lines in the Feynman diagrams concerning the original *NNN* force and evaluating the resulting two-body diagram which takes into account the in-medium modification of the nucleon propagator due to the bubble insertion. The same expression was also derived in Ref. [34] by averaging the original *NNN* force over the generalized coordinates of the third nucleon:

$$V_{\rm eff} = {\rm Tr}_{(\sigma_3,\tau_3)} \int \frac{d\boldsymbol{p}_3}{(2\pi)^3}\, n_{\boldsymbol{p}_3}\, V_{NNN}\,(1 - P_{13} - P_{23}), \qquad (11)$$

where $P_{ij} = \frac{1+\boldsymbol{\sigma}_i\cdot\boldsymbol{\sigma}_j}{2}\frac{1+\boldsymbol{\tau}_i\cdot\boldsymbol{\tau}_j}{2}P_{\boldsymbol{p}_i\leftrightarrow\boldsymbol{p}_j}$ are spin-isospin-momentum exchange operators.

I note that the $V_{\rm eff}$ as derived in Refs. [69] and [34] was obtained using the $P = 0$ approximation for total momentum of the two-nucleon pair after the average over the third particle. In addition the off-shell contribution to $V_{\rm eff}(p, p')$ was extrapolated from $V_{\rm eff}(p, p)$ by $p^2 \to \frac{p^2+p'^2}{2}$. The treatment of total momentum P was improved in Ref. [70] using a P-averaged total momentum.

In the present paper $V_{\rm eff}$ was computed using expression (11) keeping the $P = 0$ approximation. This approximation strongly simplifies the number of terms in Eq. (11). However, I want to note that especially for the case of SNM this approximation may be a strong one as discussed in Ref. [70]. In PNM instead the $P = 0$ approximation has been found to be reasonable at least for densities around normal saturation density [70]. The extension to a P-averaged total momentum is under development. One of the aims of the present work is to compare results of the calculation of the energy per particle of PNM and SNM using the approximation $p^2 \to \frac{p^2+p'^2}{2}$, denoted in the following with the label "av," with the evaluation of $V_{\rm eff}(p, p')$ without this approximation and considering both local and nonlocal regulators.

I note that, contrary to the case of local regulators [expression (6)], when using nonlocal regulators [expression (5)], the regulator function can be taken out of the integral of Eq. (11). In the case of local regulators the evaluation of Eq. (11) is much more involved.

IV. RESULTS AND DISCUSSION

This section presents the results of the calculations of the EOS, i.e., the energy per particle, E/A, as a function of the nuclear density ρ, for PNM and SNM using the models and the many-body approach described in the previous sections. Making the usual angular average of the Pauli operator and of the energy denominator [50,52], the Bethe-Goldstone equation (7) can be expanded in partial waves. In all the calculations performed in this work, I considered partial wave contributions up to a total two-body angular momentum $J_{\rm max} = 8$.

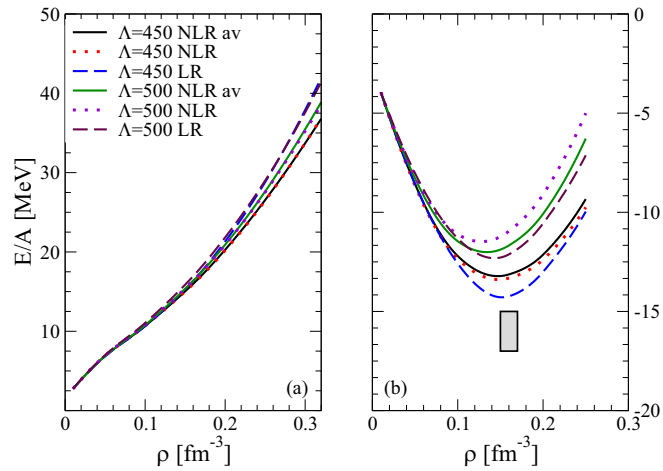

FIG. 1. Energy per particle of (a) pure neutron and (b) symmetric nuclear matter as a function of the nucleonic density for the models described in the text. Solid, dotted, and dashed lines refer to different approximations in the treatment of the *NNN* force (see text for details). The empirical saturation point of symmetric nuclear matter $\rho_0 = (0.16 \pm 0.01)\,{\rm fm}^{-3}$, $E/A|_{\rho_0} = (-16.0 \pm 1.0)\,{\rm MeV}$, is denoted by the grey box in (b).

Figure 1 shows E/A as a function of the nuclear density ρ, for PNM [Fig. 1(a)] and SNM [Fig. 1(b)], for the interactions with $\Lambda = 450$ and 500 MeV and considering different approximations in the treatment of the *NNN* force. In all the calculations shown I used two- and three-nucleon forces. I first focus on the calculations performed using a NLR. The calculations obtained by extrapolating the off-shell matrix elements in $V_{\rm eff}(p, p')$ by replacing $p^2 \to \frac{p^2+p'^2}{2}$ in $V_{\rm eff}(p, p)$ are denoted with the label "av." I note that in PNM this is a good approximation in the whole density range considered (up to $\sim 2\rho_0$) both for $\Lambda = 450$ MeV and $\Lambda = 500$ MeV. In SNM for $\Lambda = 450$ MeV the approximation is still a reasonable one since the difference between the black line which is E/A calculated in the av approximation and the dotted red line which is E/A without this approximation is $\sim$0.1 MeV in the whole density range considered. For $\Lambda = 500$ MeV I found instead that the av approximation introduces an additional binding of 0.5 MeV around saturation density. I note that the differences observed between PNM and SNM concerning the use or not of the av approximation are mainly due to the fact that the overall *NNN* contribution in PNM is typically weaker than in SNM. I now discuss the difference between the use of a LR and a nonlocal one. I remember that in both the cases the LECs are kept to the same values. In PNM E/A calculated using local regulators is always stiffer than the corresponding one obtained adopting nonlocal regulators. For $\Lambda = 450$ MeV the difference is $\sim$0.6 MeV and $\sim$3.0 MeV for $\rho = \rho_0$ and $\rho = 2\rho_0$, respectively. In SNM the use of a local

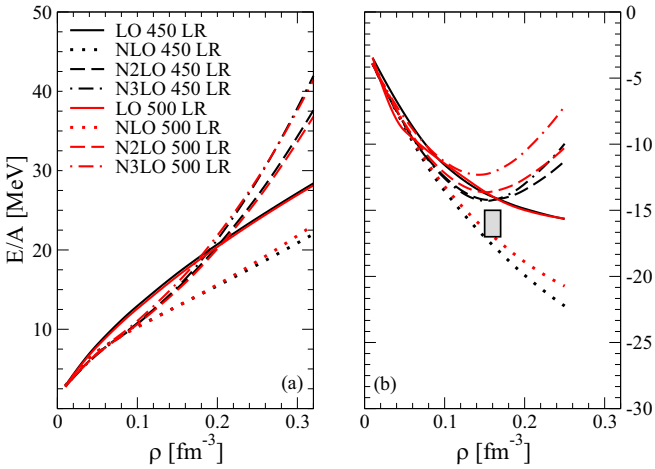

FIG. 2. Order-by-order convergence: LO, next-to-leading order (NLO), N2LO, and N3LO of energy per particle of (a) PNM and (b) SNM as a function of the nuclear density (ρ) for the models described in the text. For the *NNN* force a local regulator has been used with cutoff values of 450 MeV (black lines) and 500 MeV (red lines). The empirical saturation point of SNM, $\rho_0 = (0.16 \pm 0.01)$ fm^{-3}, $E/A|_{\rho_0} = (-16.0 \pm 1.0)$ MeV is denoted by the grey box in (b).

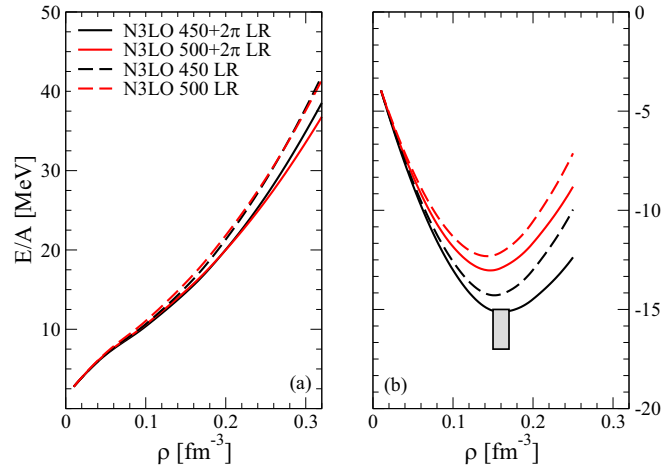

FIG. 3. Energy per particle versus nucleonic density using *NN* interactions at N3LO plus *NNN* interactions at N2LO (dashed lines). The same quantity is plotted with the inclusion of 2π-exchange processes in the *NNN* force at N3LO (continuous lines). Results are shown for two cutoff values $\Lambda = 450$ MeV (black lines) and $\Lambda = 500$ MeV (red lines). A local regulator function is adopted in all the calculations. See text for details.

regulator produces a softer E/A compared to the case in which a nonlocal regulator is employed. The energy difference is $\sim$1.1 MeV around saturation density. At larger density for the smallest cutoff the difference tends to decrease while for the largest cutoff it remains more or less constant. I checked that this behavior is mainly due to some contributions proportional to the LECs c_E and c_D which are nonvanishing using local regulators while they are zero in the case of nonlocal ones. Such terms are also isospin dependent and, thus, in some channels provide attraction while in others, repulsion. In addition I note that there is an opposite sign in the values of c_E and c_D in Table I for the two different cutoffs considered.

Figure 2 shows the convergence pattern of PNM and SNM from LO to N3LO. Although in the present calculation the contribution of the *NNN* force at N3LO is not taken into account, some interesting features can be observed. In PNM independently of the cutoff choice the calculations performed at different orders show a good convergence up to saturation density. In SNM such a pattern is similar: for $\Lambda = 450$ MeV a reasonable convergence is observed up to saturation density and then the curves show a spread; for $\Lambda = 500$ MeV the convergence seems to proceed more slowly and the energy difference at saturation density between the N2LO and the N3LO calculations is larger than 2 MeV.

To estimate the contribution of the missing diagrams of the *NNN* force at N3LO, Fig. 3 shows the energy per particle of PNM and SNM including a particular class of diagrams, namely, the 2π-exchange ones calculated up to N3LO. As discussed in Refs. [44,71] the diagrams corresponding to these processes give rise to the same analytical structure up to N4LO. Thus these contributions can be accounted for by a redefinition of low-energy constants as reported in the last two rows in Table I. The inclusion of 2π exchange produces a softening of E/A as can be clearly seen in Fig. 3 in the cases of both PNM [Fig. 3(a)] and SNM [Fig. 3(b)]. In the case of PNM for $\Lambda = 450$ MeV the additional attraction is $\sim$0.8 MeV at ρ_0 while at $2\rho_0$ it is $\sim$3 MeV; for $\Lambda = 500$ MeV at ρ_0 the attraction is $\sim$1 MeV while at $2\rho_0$ it is $\sim$4 MeV. In SNM the correction produced by the inclusion of 2π-exchange processes is of the same order of magnitude comparing with the case of PNM at saturation density. At the largest density considered in the present calculation (0.25 fm^{-3}) for the smaller (larger) cutoff I have found an attraction of $\sim$2.5 ($\sim$2.0) MeV. Clearly the inclusion of the full *NNN* force at N3LO such as that done, for instance, in Refs. [31,37] using the many-body perturbation theory is a step that should be addressed in the future. I think, however, that the previous analysis provides at least a reasonable estimate of the typical size of the missing contributions at N3LO due to the truncation of the ChPT expansion in the calculations reported in this work.

The saturation points determined by present calculations have a good saturation density in the range 0.14–0.16 fm^{-3} and values of E/A at saturation in the range -12.5 to -15.2 MeV. As shown in Fig. 3, it seems that some of the missing binding energy in E/A for model N3LO 450 LR can be recovered by including the 2π-exchange processes at N3LO. However, as I have commented before, this is just a partial consideration and the full inclusion of the N3LO force is necessary to get a better understanding.

The energy per nucleon of asymmetric nuclear matter can be accurately reproduced [72] using the so-called parabolic (in the asymmetry parameter β) approximation:

$$\frac{E}{A}(\rho,\beta) = \frac{E}{A}(\rho,0) + E_{\rm sym}(\rho)\beta^2, \qquad (12)$$

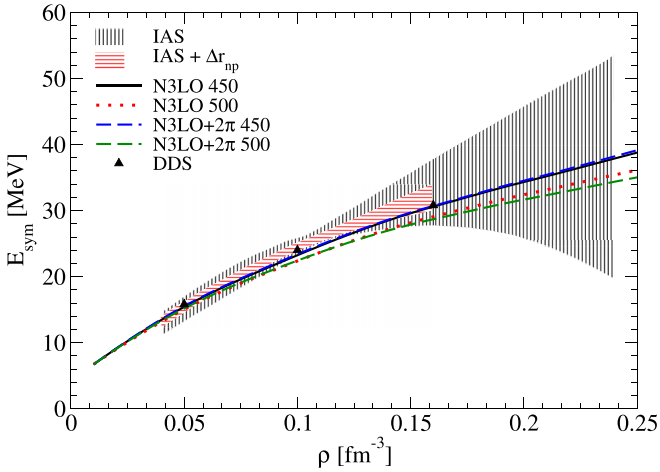

FIG. 4. Symmetry energy ($E_{\rm sym}$) versus nuclear density (ρ) for the models described in the text. The two bands represent constraints on the symmetry energy obtained by Danielewicz and Lee [76] using the excitation energies of isobaric analog states (IASs) in nuclei (black dashed band labeled IAS) and with the additional constraints from neutron skin thickness Δr_{np} of heavy nuclei [77,78] (red dashed band labeled IAS + Δr_{np}). The black triangles are the result reported in Ref. [79] based on the perturbative many-body approach (see text for details).

where $E_{\rm sym}(\rho)$ is the nuclear symmetry energy [73,74]. The nuclear symmetry energy, and in particular its density dependence, is a crucial ingredient to determine the proton fraction in β-stable nuclear matter [60] and it plays also a very important role to determine the radius and the thermal evolution of neutron stars [75]. Using Eq. (12), the symmetry energy can be calculated as the difference between the energy per particle of PNM ($\beta = 1$) and that of SNM ($\beta = 0$).

The symmetry energy, calculated within this prescription, is plotted as function of the nuclear density ρ in Fig. 4. The two bands in Fig. 4 represent the constraints on the symmetry energy obtained by Danielewicz and Lee [76] using the excitation energies of isobaric analog states (IASs) in nuclei (black dashed band labeled IAS) and with the additional constraints from the neutron skin thickness Δr_{np} of heavy nuclei [77,78] (red dashed band labeled IAS + Δr_{np}). It should be noted that the IAS constraints have been determined up to saturation density ρ_0 while at larger density they have been extrapolated [76]. In the figure is reported for comparison also the results (black triangles) of a calculation performed in Ref. [79] using low-momentum interactions at N3LO for the NN interaction and at N2LO for the three-nucleon one. I note that the inclusion or not of 2π-exchange processes at N3LO does not change appreciably the calculation of the symmetry energy. The calculations with $\Lambda = 450$ MeV show a better agreement with both the experimental constraints and the prediction of Ref. [79] than those with $\Lambda = 500$ MeV. The considered models predict values of $E_{\rm sym}$ in the range 30.6–28.5 MeV which are consistent with present constraints on this quantity.

To further compare present results with the value of the symmetry energy extracted from various nuclear experimental data [73,80], I discuss the values of the so-called slope parameter L defined as

$$L = 3\rho_0 \frac{\partial E_{\rm sym}(\rho)}{\partial \rho}\bigg|_{\rho_0} \tag{13}$$

predicted by the models considered in this work at the calculated saturation density ρ_0. The calculated values for $E_{\rm sym}(\rho_0)$ and L are compatible with the values obtained by other BHF calculations with two- and three-body interactions (see, e.g., Refs. [58,81–83]) and with the values extracted from various experimental data, $E_{\rm sym}(\rho_0) = 29.0$–$32.7$ MeV, and $L = 40.5$–61.9 MeV, as summarized in Ref. [80].

I end this section by commenting on the uncertainties in the many-body method used in this work, namely, the BHF one. As discussed in previous sections, the energy per particle in the BHF approach is calculated in a perturbative way by summing Goldstone diagrams in the hole-line expansion up to a given order. From the point of view of this expansion, it was recently shown in Ref. [84] using interactions derived in ChPT that a satisfactory convergence of the hole-line expansion is already achieved at second order, which is the same order considered in the present work. However, the analysis of Ref. [84] was carried out just considering two-body interactions. The analysis of hole-line convergence including the NNN force is still missing. However, it is plausible to expect that similar results may be obtained including the NNN force at least considering the normal ordering approximation.

A last comment concerns the inclusion of the NNN force in this approach. In addition to the approximation adopted in the average of the NNN force, a more correct treatment of the effective NNN force in the BHF approach would require the inclusion of the so-called rearrangement contribution [85,86] in the single particle potential $U_\tau(k)$. This task will be the focus of a future work.

V. SUMMARY

I have studied some approximations in the treatment of the NNN force in nuclear matter. In particular for given LECs, fixed in light nuclei calculations to reproduce the ^{3}H binding energy as well as the Gamow-Teller matrix element in ^{3}H β-decay, I compared PNM and SNM calculations in which the same local regulator employed in the few-body calculations was used, with nonconsistent calculations in which a nonlocal cutoff is instead adopted. The last case is particularly advantageous from a practical point of view because the average of the original NNN force to an effective density dependent NN one is much easier. However, I showed that this approximation leads to uncertainties larger than 1 MeV in SNM at saturation density while in pure neutron matter the use of a local or nonlocal regulator does not affect too much the calculation of the energy per particle. To estimate the theoretical uncertainty of the reported calculations due to the truncation of the NNN force at order N2LO, I performed some additional calculations including the contributions from 2π-exchange processes at N3LO in the NNN force. This inclusion is straightforward because it consists just in a redefinition of LECs due to the same analytical structure produced by 2π-exchange processes up to N4LO. I note, however, that this is just a very crude estimate

of the typical size of the terms present in the *NNN* force at N3LO and that the inclusion of the full *NNN* force at N3LO may change the numerical results. I found that this inclusion leads to a softer EOS in both SNM and PNM. The energy shift produced is about 0.5 MeV at saturation density and becomes more attractive at larger densities. I finally calculated the density behavior of the symmetry energy and compared with some experimental constraints coming from the analysis of the excitation energies in isobaric analog states combined with other constraints on neutron skin thickness in heavy nuclei. Some of the presented calculations are in good agreement with these constraints as well as with the theoretical prediction of Ref. [79] based on evolved interactions in many-body perturbation theory. I want to emphasize that the results shown in the present paper and all considerations about the accuracy and reliability in the treatment of *NNN* forces depend both on the many-body method adopted as well as on the regulation scheme employed for the *NNN* force (form of the regulator and cutoff value). In addition I note that a change of the *NN* interaction can alter the size of individual contributions of the two- and three-body forces. The next and more challenging step will be the inclusion of the full *NNN* force at N3LO and then the evaluation of three-hole-lines contribution of the BBG expansion with a consistent *NNN* force.

ACKNOWLEDGMENTS

This work is partly supported by PHAROS, COST Action CA16240. I want to thank R. Machleidt for providing me the subroutines for the *NN* interactions used in this work. A special thanks goes to Francesco Paolo Logoteta for a very useful and illuminating discussion although he was not aware of this.

[1] S. Weimberg, Physica A **96**, 327 (1979); Phys. Lett. B **251**, 288 (1990); Nucl. Phys. B **363**, 3 (1991); Phys. Lett. B **259**, 114 (1992).
[2] E. Epelbaum, Prog. Part. Nucl. Phys. **57**, 654 (2006).
[3] E. Epelbaum, H.-W. Hammer, and Ulf-G. Meißner, Rev. Mod. Phys. **81**, 1773 (2009).
[4] R. Machleidt and D. R. Entem, Phys. Rep. **503**, 1 (2011).
[5] J. W. Holt, N. Kaiser, and W. Weise, Prog. Part. Nucl. Phys. **73**, 35 (2013).
[6] N. Kalantar-Nayestanaki, E. Epelbaum, J. S. Messchendorp, and A. Nogga, Rep. Prog. Phys. **75**, 016301 (2012).
[7] H.-W. Hammer, A. Nogga, and A. Schwenk, Rev. Mod. Phys. **85**, 197 (2013).
[8] S. Binder *et al.*, Phys. Rev. C **93**, 044002 (2016).
[9] J. E. Lynn, I. Tews, J. Carlson, S. Gandolfi, A. Gezerlis, K. E. Schmidt, and A. Schwenk, Phys. Rev. C **96**, 054007 (2017).
[10] D. Lonardoni, J. Carlson, S. Gandolfi, J. E. Lynn, K. E. Schmidt, A. Schwenk, and X. B. Wang, Phys. Rev. Lett. **120**, 122502 (2018).
[11] A. Ekström, G. R. Jansen, K. A. Wendt, G. Hagen, T. Papenbrock, B. D. Carlsson, C. Forssén, M. Hjorth-Jensen, P. Navrátil, and W. Nazarewicz, Phys. Rev. C **91**, 051301(R) (2015).
[12] R. Roth, S. Binder, K. Vobig, A. Calci, J. Langhammer, and P. Navrátil, Phys. Rev. Lett. **109**, 052501 (2012).
[13] D. Lonardoni, S. Gandolfi, J. E. Lynn, C. Petrie, J. Carlson, and K. E. Schmidt, and A. Schwenk, Phys. Rev. C **97**, 044318 (2018).
[14] S. Binder, J. Langhammer, A. Calci, and R. Roth, Phys. Lett. B **736**, 119 (2014).
[15] R. J. Furnstahl, D. R. Phillips, and S. Wesolowski, J. Phys. G **42**, 034028 (2015).
[16] D. R. Entem, R. Machleidt, and Y. Nosyk, Phys. Rev. C **96**, 024004 (2017).
[17] E. Epelbaum, A. Nogga, W. Glöckle, H. Kamada, and Ulf-G. Meißner, and H. Witała, Phys. Rev. C **66**, 064001 (2002).
[18] B. D. Day, Rev. Mod. Phys. **39**, 719 (1967).
[19] M. Baldo and G. F. Burgio, Rep. Prog. Phys. **75**, 026301 (2012).
[20] D. Logoteta, I. Vidana, I. Bombaci, and A. Kievsky, Phys. Rev. C **91**, 064001 (2015).
[21] D. Logoteta, I. Bombaci, and A. Kievsky, Phys. Lett. B **758**, 449 (2016).
[22] D. Logoteta, I. Bombaci, and A. Kievsky, Phys. Rev. C **94**, 064001 (2016).
[23] A. Kievsky, M. Viviani, D. Logoteta, I. Bombaci, and L. Girlanda, Phys. Rev. Lett. **121**, 072701 (2018).
[24] K. Hebeler and A. Schwenk, Phys. Rev. C **82**, 014314 (2010).
[25] I. Tews, T. Krüger, K. Hebeler, and A. Schwenk, Phys. Rev. Lett. **110**, 032504 (2013).
[26] A. Roggero, A. Mukherjee, and F. Pederiva, Phys. Rev. Lett. **112**, 221103 (2014).
[27] G. Wlazlowski, J. W. Holt, S. Moroz, A. Bulgac, and K. J. Roche, Phys. Rev. Lett. **113**, 182503 (2014).
[28] S. Gandolfi, A. Gezerlis, and J. Carlson, Annu. Rev. Nucl. Part. Sci. **65**, 303 (2015).
[29] I. Tews, S. Gandolfi, A. Gezerlis, and A. Schwenk, Phys. Rev. C **93**, 024305 (2016).
[30] K. Hebeler and A. Schwenk, Eur. Phys. J. A **50**, 11 (2014).
[31] C. Drischler, A. Carbone, K. Hebeler, and A. Schwenk, Phys. Rev. C **94**, 054307 (2016).
[32] K. Hebeler, S. K. Bogner, R. J. Furnstahl, A. Nogga, and A. Schwenk, Phys. Rev. C **83**, 031301(R) (2011).
[33] Z. H. Li and H.-J. Schulze, Phys. Rev. C **85**, 064002 (2012).
[34] A. Carbone, A. Polls, and A. Rios, Phys. Rev. C **88**, 044302 (2013).
[35] L. Coraggio, J. W. Holt, N. Itaco, R. Machleidt, L. E. Marcucci, and F. Sammarruca, Phys. Rev. C **89**, 044321 (2014).
[36] M. Kohno, Prog. Theor. Exp. Phys. **2015**, 123D02 (2015).
[37] C. Drischler, K. Hebeler, and A. Schwenk, Phys. Rev. Lett. **122**, 042501 (2019).
[38] E. Epelbaum, H. Krebs, and U.-G. Meißner, Phys. Rev. Lett. **115**, 122301 (2015).
[39] D. R. Entem, N. Kaiser, R. Machleidt, and Y. Nosyk, Phys. Rev. C **92**, 064001 (2015).
[40] M. Piarulli, L. Girlanda, R. Schiavilla, A. Kievsky, A. Lovato, L. E. Marcucci, S. C. Pieper, M. Viviani, and R. B. Wiringa, Phys. Rev. C **94**, 054007 (2016).
[41] M. Piarulli, L. Girlanda, R. Schiavilla, R. N. Pérez, J. E. Amaro, and E. R. Arriola, Phys. Rev. C **91**, 024003 (2015).

[42] L. Girlanda, A. Kievsky, and M. Viviani, Phys. Rev. C **84**, 014001 (2011).
[43] M. Hoferichter, J. Ruiz de Elvira, B. Kubis, and Ulf-G. Meissner, Phys. Rev. Lett. **115**, 192301 (2015); Phys. Rep. **625**, 1 (2016).
[44] F. Sammarruca, L. E. Marcucci, L. Coraggio, J. W. Holt, N. Itaco, and R. Machleidt, arXiv:1807.06640.
[45] L. E. Marcucci, F. Sammarruca, M. Viviani, and R. Machleidt, Phys. Rev. C **99**, 034003 (2019).
[46] R. Schiavilla (unpublished).
[47] L. E. Marcucci, A. Kievsky, S. Rosati, R. Schiavilla, and M. Viviani, Phys. Rev. Lett. **121**, 049901(E) (2018).
[48] M. Piarulli, L. Girlanda, R. Schiavilla, R. N. Perez, J. E. Amaro, and E. R. Arriola, Phys. Rev. C **85**, 024003 (2012).
[49] J. P. Jeukenne, A. Lejeunne, and C. Mahaux, Phys. Rep. **25**, 83 (1976).
[50] P. Grangé, J. Cugnon, and A. Lejeune, Nucl. Phys. A **473**, 365 (1987).
[51] M. Baldo, I. Bombaci, G. Giansiracusa, U. Lombardo, C. Mahaux, and R. Sartor, Phys. Rev. C **41**, 1748 (1990).
[52] M. Baldo, I. Bombaci, L. S. Ferreira, G. Giansiracusa, and U. Lombardo, Phys. Rev. C **43**, 2605 (1991).
[53] H. Q. Song, M. Baldo, G. Giansiracusa, and U. Lombardo, Phys. Rev. Lett. **81**, 1584 (1998).
[54] M. Baldo, G. Giansiracusa, U. Lombardo, and H. Q. Song, Phys. Lett. B **473**, 1 (2000).
[55] M. Baldo, I. Bombaci, G. Giansiracusa, and U. Lombardo, J. Phys. G: Nucl. Part. Phys. **16**, L263 (1990).
[56] F. Coester, S. Cohen, B. Day, and C. M. Vincent, Phys. Rev. C **1**, 769 (1970).
[57] B. Day, Phys. Rev. Lett. **47**, 226 (1981).
[58] Z. H. Li, U. Lombardo, H.-J. Schulze, W. Zuo, L. W. Chen, and H. R. Ma, Phys. Rev. C **74**, 047304 (2006).
[59] B. Friedman and V. R. Pandharipande, Nucl. Phys. A **361**, 502 (1981).
[60] M. Baldo, I. Bombaci, and G. F. Burgio, Astron. Astrophys. **328**, 274 (1997).
[61] A. Akmal, V. R. Pandharipande, and D. G. Ravenhall, Phys. Rev. C **58**, 1804 (1998).
[62] Z. H. Li, U. Lombardo, H. J. Schulze, and W. Zuo, Phys. Rev. C **77**, 034316 (2008).
[63] G. Taranto, M. Baldo, and G. F. Burgio, Phys. Rev. C **87**, 045803 (2013).
[64] W. Zuo, I. Bombaci, and U. Lombardo, Eur. Phys. J. A **50**, 12 (2014).
[65] H. A. Bethe, Phys. Rev. **138**, B804 (1965).
[66] R. Rajaraman and H. A. Bethe, Rev. Mod. Phys. **39**, 745 (1967).
[67] B. A. Loiseau, Y. Nogami, and C. K. Ross, Nucl. Phys. A **401**, 601 (1971).
[68] P. Grangé, A. Lejeune, M. Martzolff, and J.-F. Mathiot, Phys. Rev. C **40**, 1040 (1989).
[69] J. W. Holt, N. Kaiser, and W. Weise, Phys. Rev. C **81**, 024002 (2010).
[70] C. Drischler, K. Hebeler, and A. Schwenk, Phys. Rev. C **93**, 054314 (2016).
[71] H. Krebs, A. Gasparyan, and E. Epelbaum, Phys. Rev. C **85**, 054006 (2012).
[72] I. Bombaci and U. Lombardo, Phys. Rev. C **44**, 1892 (1991).
[73] B. A. Li, A. Ramos, G. Verde, and I. Vidaña, Eur. Phys. J. A **50**, 9 (2014).
[74] M. Baldo and G. F. Burgio, Prog. Part. Nucl. Phys. **91**, 203 (2016).
[75] A. W. Steiner, Phys. Rev. C **74**, 045808 (2006).
[76] P. Danielewicz and J. Lee, Nucl. Phys. A **922**, 1 (2014).
[77] X. Roca-Maza, M. Brenna, B. K. Agrawal, P. F. Bortignon, G. Colo, L. G. Cao, N. Paar, and D. Vretenar, Phys. Rev. C **87**, 034301 (2013).
[78] Z. Zhang and L.-W. Chen, Phys. Lett. B **726**, 234 (2013).
[79] C. Drischler, V. Somà, and A. Schwenk, Phys. Rev. C **89**, 025806 (2014).
[80] J. M. Lattimer, Gen. Relativ. Gravitation **46**, 1713 (2014).
[81] Z. H. Li and H.-J. Schulze, Phys. Rev. C **78**, 028801 (2008).
[82] I. Vidaña, C. Providência, A. Polls, and A. Rios, Phys. Rev. C **80**, 045806 (2009).
[83] I. Vidaña, A. Polls, and C. Providência, Phys. Rev. C **84**, 062801(R) (2011).
[84] J.-J. Lu, Z.-H. Li, C.-Y. Chen, M. Baldo, and H.-J. Schulze, Phys. Rev. C **96**, 044309 (2017).
[85] W. Zuo, I. Bombaci, and U. Lombardo, Phys. Rev. C **60**, 024605 (1999).
[86] A. H. Lippok and H. Müther, Phys. Rev. C **92**, 034312 (2015).